Laminar Burning Velocities of Methane -air Mixtures at Elevated Pressures and Temperatures

Robin John Varghese * Harshal Kolekar B. Aravind Sudarshan Kumar
Indian Institute of Technology Bombay
Mumbai, Maharashtra, India

1 Introduction

The depletion of fossil fuels and stringent emission norms are leading combustion research in the direction of environment-friendly alternatives for power generation and transportation. Integrated Gasification and Combined Cycle (IGCC), power plants for electricity, aim in the reduction of the carbonaceous emissions and NO_x emissions by using Carbon Capture Storage technique and lean premixed combustion respectively. Recently, IGCC using natural gas has gained more attention due to the clean burning of these gaseous fuels compared to the producer gas mixtures used widely. Natural gas reserves are abundant and have untapped potential in meeting the power demand as well as in internal combustion engines with better emission control. Land-based gas turbine engines for power generation could attain better performance with natural gas.

For understanding the fundamental combustion characteristics in terms of ignition delay, flame propagation speed, flame instabilities, and dynamic behaviors, methane is extensively used. Burning velocity or flame speed is one such property that has been studied in detail that gives the overall reaction rate of the fuel-air mixture as a concise entity. Laminar burning velocity in conjunction with the ignition delay characteristics is used for validation of detailed chemical kinetic schemes. Laminar burning velocity is one of the critical parameters that determine flashback and lift off.

The various techniques for measurement of laminar burning velocity with steady and dynamic flame propagation are spherically expanding flames (SEF) [1–3], heat-flux method [4, 5], counter-flow stagnation method [6, 7]. Hinton et al. [1] determined the burning velocities at higher pressures and temperatures using spherically expanding flames. Zhu et al. [7] measured flame speeds of methane / (Ar, N_2, CO_2) using the counterflow technique. Liao et al. [2] presented the burning velocities and Markstein numbers of spherically expanding flames of methane-air at different initial pressures. In the methods discussed above, all use the experimental data obtained and either extrapolate to adiabatic or zero strain rate conditions to obtain the laminar burning velocity. Chen et al. [8] presented a review of measured flame speeds of methane-air mixtures using spherically expanding flames. They suggested the use of flame speed data from the method

Correspondence to: robinjohnvarghese@gmail.com

should be utilized for reducing the uncertainty of chemical models primarily at elevated pressures. The preheated diverging channel technique used in this study does not use any such data reduction procedures. On the other hand, the method provides burning velocities for a range of elevated temperatures ($350 - 650\ K$).

Extensive research on the fundamental combustion parameter of methane-air flames is available. However, investigation of the combined effect of elevated pressures and temperatures on the laminar burning velocity is limited. The preheated diverging channel method regarded as an accurate method for capturing the flame velocities at elevated temperatures [9, 10] has been extended to higher pressures. The experimental measurements for methane-air mixtures for different equivalence ratios ($\phi = 0.7 - 1.3$) are reported for 2 atm, and elevated temperatures of $350 - 650K$. The temperature exponents of the mixtures are also presented. Chemical kinetic simulations using two kinetic schemes (GRI-Mech 3.0 [11], and Foundational Fuel Chemistry Model- FFCM-1 [12]) have also been compared with the experiments.

2 Experimental details

The preheated diverging channel method for measurement of laminar burning velocities [9] are housed inside the cylindrical pressure vessel ($40\ L$) as shown in Fig. 1 Right. A viewing window (toughened glass) is provided on the top of the pressure vessel for observing the stabilized flames, and capturing the images of the flame using a DSLR camera. The top part of the vessel holds the pressure relief valve and a pressure gauge. The infrared heater is placed below the diverging channel at a distance of $2\ cm$, and horizontal overlap of $2\ cm$. An ignition device is placed at the exit of the diverging channel. A k-type thermocouple is used for temperature measurements at various heating rates and different flow rates. The thermocouple could be moved with the help of a traverse mechanism along the length of the channel ($0 - 7\ cm$ from the exit of the channel). The tip of the thermocouple is bent towards the inside lower wall of the channel. The temperature profile of the channel inside the chamber is measured at various inlet velocities (cold flow) beforehand at different preheat conditions. The chamber is provided with three air inlets (one at the bottom, two at the top) for pressurizing the vessel. The pressure relief valve controls the pressure inside the chamber and is accurate up to $\pm\ 0.05\ atm$ of the indicated value in the pressure gauge.

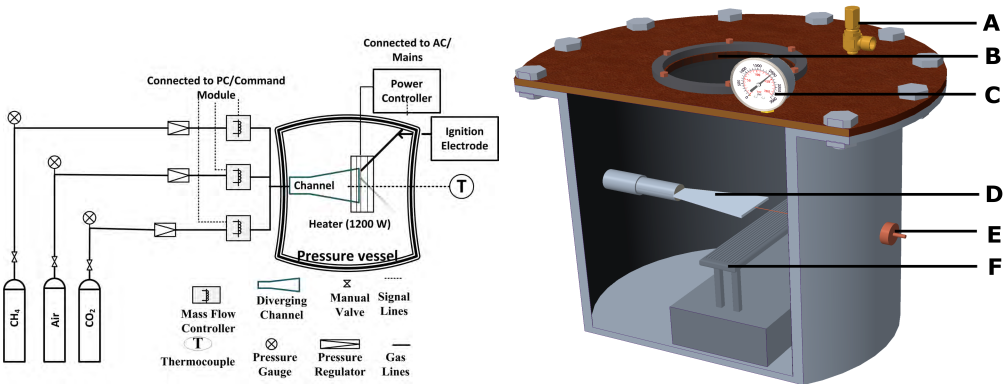

Figure 1: Left: Schematic of the experimental facility, Right: High-pressure vessel, sectional view; A - Pressure relief valve, B - Glass window, C- Pressure gauge, D - Diverging channel, E - Thermocouple, F - Infrared heater.

Figure 1 shows the schematic of the experimental facility. The mesoscale channel provides a uniform ve-

locity field and the divergence aids in preventing flashback [9]. The incoming mixture is preheated with a super high-temperature heater of $1200\ W$, which provides a positive temperature gradient along the axial direction. The positive temperature gradient helps in the stabilization of the planar flames [9]. The mixture equivalence ratio and flow velocity inside the channel is precisely controlled and monitored using the coupled system of Mass Flow Controllers (MFC), a command module, and a computer.

The experiments were carried out for different preheat temperatures and equivalence ratios ($\phi = 0.7 - 1.3$). Initially, the cylindrical vessel is filled with air at a pressure of $2\ atm$, and the relief valve controls the pressure. The infrared heater is turned on at the required ($600 - 1000\ W$) heating rate. The infrared heater has a response time of a few minutes, and on reaching the steady state, the premixed fuel-air mixture is fed into the channel using MFCs. The ignition device is switched on, and the flame is established inside the channel. The flame moves inside the channel gradually and stabilizes at a position where the flow velocity matches the local laminar burning velocity. The exhaust products fill inside the $40\ L$ chamber and are pushed out through the relief valve after mixing with the pressurized air inside the chamber. Since the products are $\approx\ 5\ \%$ of the volume of the chamber, the properties of the stabilized flames are unaffected. The properties of the stabilized flames (flame area and unburnt gas temperature) are used for the determination of laminar burning velocity at various temperatures using a rearranged form of mass conservation equation. $S_u = U_{inlet} \times \frac{A_{inlet}}{A_f} \times \frac{T_u}{T_{u,o}}$, where U_{inlet} is the mixture inlet velocity, A_{inlet} area of the channel inlet, A_f channel area at the flame location point, $T_{u,o}$ is the mixture temperature at the channel inlet, and T_u is the unburnt mixture temperature at the flame stabilization location. A_f is determined from the position of the planar flame.

3 Results and discussion

The high-temperature heater gives a positive temperature gradient inside the diverging channel. The channel wall temperatures are measured at several flow velocities of air mixtures at different locations inside the channel. The mixture is assumed to have the same temperature as that of the temperature of the wall. The flame stabilizes at various positions for a particular equivalence ratio depending on the inlet velocity and the temperature distribution in the channel. The details on the calculation of burning velocity can be found elsewhere [9]. Figure 2, Right shows the stabilized flame formed inside the diverging channel for methane-air mixture ($\phi = 1.0$) at an inlet velocity, $U_{in} = 0.8m/s$.

Figure 2 Left Shows the variation of burning velocities for various high preheat temperatures for two particular equivalence ratios ($\phi = 0.7, 1.0$). The burning velocity increases with an increase in preheat temperature since the enthalpy of the reactant mixture is higher. The unburnt mixture temperature before the flame is at a higher enthalpy compared to the ambient conditions. The increased energy content increases the adiabatic flame temperature of these mixtures. The measured burning velocities are in good agreement with the experiments performed by [13,14,16] for stoichiometric mixtures with a slight overprediction compared to Clarke and Stone [15]. Figure 2 Left also shows the comparison with the simulations using the kinetic scheme GRI-Mech 3.0. The GRI-Mech 3.0, and FFCM-1 simulations marginally underpredict the laminar burning velocities at all temperatures for both lean and stoichiometric mixtures. The comparison with previous literature shows relatively similar burning velocities. The inset table of Fig. 2 Left shows the power law fit parameters and the equation. The laminar burning velocity at $300\ K$ and the temperature exponent for both equivalence ratios are also shown in the figure.

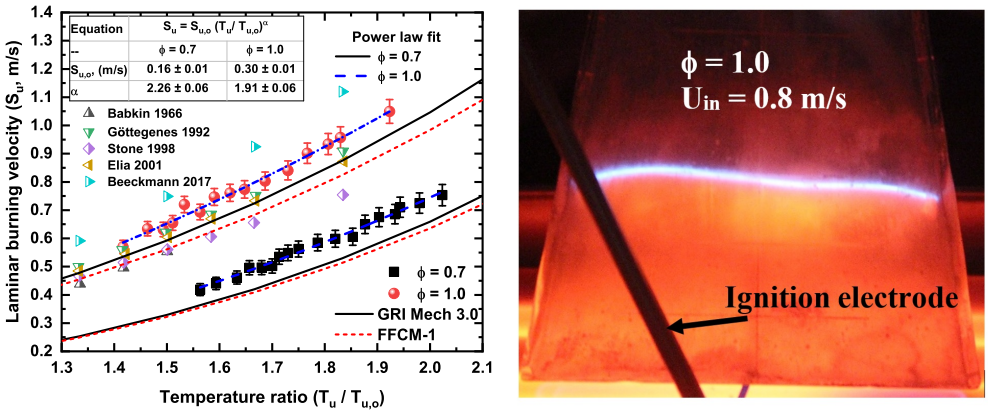

Figure 2: Left: Variation of burning velocity for two different equivalence ratios ($\phi = 0.7, 1.0$), comparison with the literature [13–16] and kinetic simulations; Right: Stabilized flame in the diverging channel at an inlet velocity 0.8 m/s, and stoichiometric methane-air mixture.

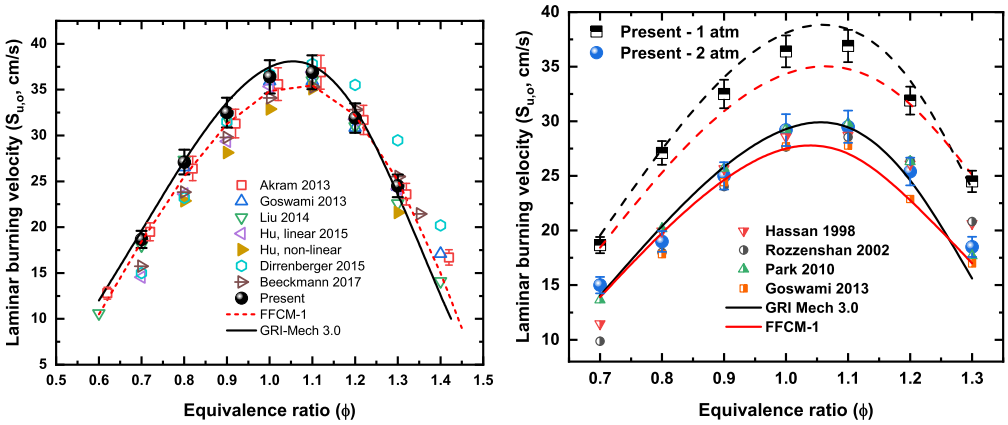

Figure 3: Left: Comparison of the laminar burning velocity for the methane-air mixture measured at 1 atm, and 300 K with the literature [4, 17–19], Right: Comparison of burning velocities of methane-air mixtures at 2 atm H Symbols: experiments, lines: simulations using PREMIX.

The laminar burning velocities of previous experiments using diverging channel method are compared in Fig. 3 Left with the burning velocities of methane-air mixtures at 300 K and 1 atm in available literature. The present results are in excellent agreement with various measurement techniques and simulations using two different kinetic schemes (GRI-Mech 3.0 and FFCM-1). Figure 3, Right shows the variation of laminar burning velocity for various equivalence ratios at an elevated pressure of 2 atm. The decrease of the burning velocities with the increase in pressure is evident in Fig. 3. The present results match well with different available data [4, 17–19] in the literature. The numerical predictions using the GRI-Mech 3.0 mechanism also shows the burning velocities comparable to the experimental values. The planar flames stabilized in these channels provides accurate values of laminar burning velocities [9]. The small divergence angle (10^o) and low flow rates of fuel and air leads to negligible strain in the flow ($30 - 50\ s^{-1}$) [9]. The flame area determined has an uncertainty of $\pm$ 0.71 mm^2. The uncertainty analysis considering the effect of various parameters obscures the results by $\pm$ 5 % [9]. The uncertainty of burning velocities measured using the

diverging channel method is discussed in detail in [9, 10].

Figure 4 Left shows the temperature exponents obtained from the determined laminar burning velocities at various equivalence ratios. The procedure shown in Fig. 2, Left is repeated for different equivalence ratios to obtain the temperature exponents. The temperature exponents obtained from the previous measurements at 1 atm is also included to compare the effect of pressure on the temperature exponents. The temperature exponents slightly increase with pressure for all the equivalence ratios presented. Non-monotonic behavior shown for 1 atm conditions with a minimum at slightly rich mixtures is followed at a higher pressure of 2 atm as well. The comparison from previous research studies is within $\pm$ 5 $\%$ for the present stoichiometric measurements. The predictions using GRI-Mech 3.0 agree well with the present experiments.

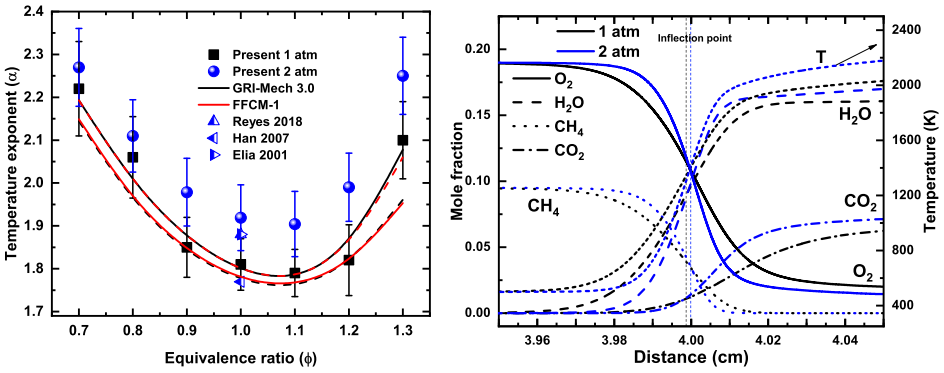

Figure 4: Left: Variation of temperature exponents at different equivalence ratios. Symbols: experiments, lines: simulations using PREMIX., Right: Species mole fraction near the flame position using kinetic predictions of GRI-Mech 3.0.

Figure 4 shows the species mole fractions of major species and temperature variation near the flame position for 1 atm, and 2 atm methane-air stoichiometric flames with an unburnt gas temperature of 500 K. The flame temperature at equilibrium is slightly higher for elevated pressures. Species mole fractions at equilibrium are also slightly higher at elevated pressures of 2 atm. However, the flame position shifts slightly upstream and indicating the slower reaction rate. The reduction in species mole fractions of CH_4, O_2 and the formation of H_2O, CO_2 is delayed by 0.01 mm for the higher pressure case. The predicted burning velocity of 2 atm, 1 atm methane-air at 500 K using GRI-Mech 3.0 is 72 cm/s, 91 cm/s respectively. A comprehensive study on the sensitivity of various reactions and ROP of the radicals would yield a complete understanding of the reduction in burning velocity from the aspect of reaction kinetics.

4 Conclusions

Measurements of the laminar burning velocities of methane were conducted over a range of equivalence ratios ($\phi = 0.7 - 1.3$) at elevated pressures of 2 atm for a temperature range of 350-600 K The properties of planar flames stabilized in the channel were used for determination of laminar burning velocities. The laminar burning velocities increase with the increase in mixture temperature due to the higher reactant enthalpy. The laminar burning velocities of methane-air mixtures at 2 atm follow the non-monotonic behavior of the burning velocities at 1 atm with a maximum at $\phi = 1.1$. The comparison with the results obtained from

the experiments matches with the PREMIX calculations using GRI-Mech 3.0 mechanism. The temperature exponents for a range of equivalence ratios ($\phi = 0.7 - 1.3$) were also discussed. The burning velocity measurements at elevated pressures and temperatures are scarce, and since the temperature exponents were compared only for stoichiometric mixtures. Generally, the burning velocity and temperature exponents from the present measurements agree well with recent literature and GRI-Mech 3.0 calculations. The extension of the existing method for measurements at elevated pressures was validated with the laminar burning velocities of methane obtained using the high pressure preheated diverging channel technique. The potential for measurements at elevated pressures and temperatures using the method could mean accurate measurements that comprehensively study the combined effect of elevated pressures and temperatures on burning velocities.

References

[1] N. Hinton, R. Stone, Fuel 116 (2014) 743–750.

[2] S. Y. Liao, D. M. Jiang, J. Gao, Z. H. Huang, Energy Fuel 18 (2) (2004) 316–326.

[3] C. Prathap, A. Ray, M. R. Ravi, Combust. Flame 155 (1-2) (2008) 145–160.

[4] M. Goswami, S. C. R. Derks, K. Coumans, W. J. Slikker, M. H. de Andrade Oliveira, R. J. M. Bastiaans, C. C. M. Luijten, L. P. H. de Goey, A. A. Konnov, Combust. Flame 160 (9) (2013) 1627–1635.

[5] A. A. Konnov, I. V. Dyakov, Exp. Therm. Fluid Sci. 29 (8) (2005) 901–907.

[6] T. T. Leach, C. P. Cadou, G. S. Jackson, Combust. Theory Model. 10 (1) (2006) 85–103.

[7] D. L. Zhu, F. N. Egolfopoulos, C. K. Law, Symp. (Int.) Combust. 22 (1) (1989) 1537–1545.

[8] Z. Chen, Combust. Flame 162 (6) (2015) 2442–2453.

[9] R. J. Varghese, H. Kolekar, V. Hariharan, S. Kumar, Fuel 214 (October 2017) (2018) 144–153.

[10] R. J. Varghese, H. Kolekar, S. Kumar, Int. J. Hydrogen Energy (2019) in press.

[11] G. P. Smith, D. M. Golden, M. Frenklach, N. W. Moriarty, B. Eiteneer, M. Goldenberg, C. T. Bowman, R. K. Hanson, S. Song, W. C. Gardiner Jr, GRI-Mech 3.0.

[12] G. P. Smith, Y. Tao, H. Wang, Foundational Fuel Chemistry Model Version 1.0 (FFCM-1).

[13] V. S. Babkin, L. S. Kozachenko, Combust. Explos. Shock Waves 2 (3) (1966) 46–52.

[14] J. Göttgens, F. Mauss, N. Peters, Symp. (Int.) Combust. 24 (1) (1992) 129–135.

[15] R. Stone, A. Clarke, P. Beckwith, Combust. Flame 114 (3-4) (1998) 546–555.

[16] M. Elia, M. Ulinski, M. Metghalchi, J. Eng. Gas Turb. Power 123 (1) (2001) 190–196.

[17] M. I. Hassan, K. T. Aung, G. M. Faeth, Combust. Flame 115 (4) (1998) 539–550.

[18] G. Rozenchan, D. L. Zhu, C. K. Law, S. D. Tse, Proc. Combust. Inst. 29 (2) (2002) 1461–1470.

[19] O. Park, P. S. Veloo, N. Liu, F. N. Egolfopoulos, Proc. Combust. Inst. 33 (1) (2011) 887–894.